Printed in U.S.A.

69-HT-28

an ASME publication

Stability of Cylindrical Bubbles in a Vertical Pipe

Y. Y. HSU
F. F. SIMON
Lewis Research Center,
National Aeronautics and Space Administration,
Cleveland, Ohio

The stability of cylindrical bubbles rising in vertical pipes of various diameters (1.27 to 30 cm) is studied photographically. Single cylindrical bubbles remain stable in pipes of all sizes for durations up to 10 to 20 seconds, provided that the flow field is quiescent. Bubble-splitting occurs when the bubble is in the presence of disturbances such as pressure pulsation, convection cells, or the wake of a leading bubble. The wake effect is studied in detail. The critical bubble spacing for instability increases with the square of the diameter.

Contributed by the Heat Transfer Division of The American Society of Mechanical Engineers for presentation at the ASME-AIChE Heat Transfer Conference, Minneapolis, Minn., August 3-6, 1969. Manuscript received at ASME Headquarters May 12, 1969.

Copies will be available until June 1, 1969.

Stability of Cylindrical Bubbles in a Vertical Pipe

Y. Y. HSU F. F. SIMON

ABSTRACT

The stability of cylindrical bubbles rising in vertical pipes of various diameters (1.27 to 30 cm) is studied photographically. Single cylindrical bubbles remain stable in pipes of all sizes for durations up to 10 to 20 seconds, provided that the flow field is quiescent. Bubble-splitting occurs when the bubble is in the presence of disturbances such as pressure pulsation, convection cells, or the wake of a leading bubble. The wake effect is studied in detail. The critical bubble spacing for instability increases with the square of the diameter.

NOMENCLATURE

A	area
A_1, A_2, B_1, B_2	coefficients for velocity potential function
a	pipe radius
c	constant
D	diameter of pipe
g	gravitational acceleration
J_o, J_1	Bessel functions of zeroth and first order
k	wave number
L	length of a bubble or a slug, or a wake
N	$N = L_w/D$
p	pressure
p_o	steady state pressure
Q	volumetric flow rate
r	distance from pipe centerline
t	time
u	velocity
V	volume
w	wave period
x	vertical coordinate
α	number such that $J_1(\alpha a) = 0$
δ	film thickness
η	displacement due to disturbance $x_i - x_{oi}$
λ	wavelength
ν	kinematic viscosity
Ω	vorticity
φ	potential function
Ψ	stream function
ρ	density
$\Delta\rho$	$\rho - \rho'$
σ	interfacial tension

Subscript:

b	bubble
c	critical spacing, also critical wavelength
d	most dangerous
g	gas
l	liquid
m,n	order of roots for the Bessel function $J_1(ka)$
o	reference condition
r	radius
v	vapor
w	wake
x	x-direction

i gas-liquid interface at infinite distance

1 steady state

2 perturbation

Superscript:

* critical size

' refer to vapor phase

INTRODUCTION

Among the various flow patterns encountered in two-phase flow, slug flow is of particular interest because of its association with pressure pulsations. It would be useful if the limiting conditions for the existence of slug flow in a particular pipe could be determined. Since slug flow is a train of cylindrical bubbles with spherical caps (or Taylor bubbles, Ref. (2)) flowing in succession, one should first examine the individual bubbles. Information obtained concerning the behavior of the individual Taylor bubbles, the stability limit of a single bubble, and the interaction between succeeding bubbles can be used to draw up the stability criteria for slug flow. This study attempts to determine:

1. The critical size of a stable single bubble.
2. The effect of disturbances on the stability of a Taylor bubble, particularly the wake effect of a preceding bubble.
3. The critical spacing between the stable bubbles as a function of the pipe diameter.

A motion picture supplement accompanies this report to help illustrate the findings. To familiarize the reader with the types of bubbles and flows to be discussed typical views of a stable Taylor bubble, an unstable Taylor bubble, stable slug flow and unstable slug flow (transitioning into churn-bubbly flow) are shown in Figs. 1(a), 1(b), 2(a), and 2(b), respectively.

LITERATURE SURVEY

The hydrodynamics of long stable bubbles in a pipe has been the subject of many studies. The rising velocity of a bubble in a vertical pipe was found to be directly proportional to the squre root of the diameter. Values of the

$$u = C\sqrt{Dg} \tag{1}$$

coefficient C were proposed by Davies and Taylor (Ref. (2)) and Dumitrescu (Ref. (3)) and were found to be a function of bubble Reynolds number and pipe Reynolds number according to Griffith and Wallis (Ref. (4)). The case of a rising plane bubble was studied by Birkoff and Carter (Ref. (5)), Garabedian (Ref. (6)), and Collins (Ref. (7)). Collins also related the rising velocity of a large cap bubble to the bubble volume and the wall effect (Ref. (8)). Davies and Taylor (Ref. (2)) studied the effect of flow field on bubble shape, based upon an earlier work of Taylor (Ref. (9)). The shape of and the film flow around a Taylor bubble were studied by Brown (Ref. (10)) by considering viscosity effects. Bretherton (Ref. (11)) proposed a criterion to determine whether or not a bubble will rise in a capillary tube. A stability criterion has been proposed by Goldsmith and Mason (Ref. (12)) for the breakup of the tail end of a long bubble.

In the area of slug flow, the kinematic relation of the bubbles and the liquid flow was studied by Street and Tek (Ref. (13)) and by Nicklin, Wilke, and Davidson (Ref. (14)). It was suggested that the bubble velocity is $u_b = 1.24\,(Qg + Q_1)/A + 0.35\sqrt{gD}$ according to the measurement of Nicolitsas and Murgatroyd (Ref. (15)).

A picture of the wake of a large cap bubble showing strong vorticity was published by Slaughter and Wraith (Ref. (16)). The circulation of a bubble wake was found to be approximately $3\sqrt{gV}$ according to Walters and Davidson (Ref. (17)). Detailed measurements of velocity profiles in the wake of Taylor bubbles were done by Moissis and Griffith (Ref. (18)). Their results showed that the wake effect decayed rapidly within 3-5 diameters from the tail end of the bubble. Moissis (Ref. (19)) further extended his study to give a criterion for the limiting vapor flow rate of slug flow.

The instability at the interface between two fluids of different densities with the heavier fluid being accelerated toward the lighter fluid is known as a Taylor instability (Ref. (1)). It was shown by Taylor that if a two-dimensional flat surface is unstable, the critical wavelength is $\lambda_c = 2\pi\sqrt{\sigma/g(\rho_1 - \rho_v)}$. Bellman and Pennington (Ref. (20)) later showed that for the condition of maximum growth rate, the critical wavelength (or "the most dangerous wavelength") is $\lambda_d = 2\sqrt{3}\,\pi\sqrt{\sigma/g(\rho_1 - \rho_v)}$.

THEORETICAL ANALYSIS FOR SINGLE BUBBLE

In the present study a small perturbation will be mathematically imposed on the steady-state velocity potential function and the profile of a bubble moving in a vertical pipe. A critical condition will be established to determine if such a perturbation will grow or decay with time. This critical condition will be used as the criterion for bubble stability. A detailed derivation can be found in Ref. (21). Only a general outline of the approach will be sketched here.

The steady-state velocity potential of a liquid in relative motion with a bubble confined in a vertical pipe was proposed by Davies and Taylor (Ref. (2)) as follows:

$$\varphi_1 = -u_\infty x + \sum_{n=1}^{\infty} A_{1n} e^{\alpha_n x} J_o(\alpha_n r) \tag{2}$$

The coordinates and symbols are shown in Fig. 3. Note that the coordinate is fixed with respect to the bubble, i.e., the bubble is considered stationary while the liquid moves toward the bubble at a velocity u_∞, which is actually the rising velocity of the bubble.

The value of α_n is such that $J_1(\alpha_n a) = 0$ to satisfy the boundary condition that

$$u_r = -\frac{\partial \varphi_1}{\partial r} = \sum_{n=1}^{\infty} A_{1n} e^{\alpha_n x_i} \alpha J_1(\alpha_n r) \quad (3a)$$

vanishes at $r = a$.

The evaluation of the A_{1n} corresponding to α_n requires the matching of one boundary condition for each α_n. Davies and Taylor only tried to match the boundary condition at the stagnation point, and thus, only the first nonvanishing root of the Bessel function $J_1(\alpha_n a)$ was retained. This approximation was found to be sufficiently accurate (Ref. (2)). The first root of the Bessel function is in the neighborhood of the stagnation point.

$$\alpha_1 = \frac{3.832}{a} \quad (4)$$

Accordingly, in Ref. (2), only the first terms in the summation were retained (the subscript n is dropped) and Eqs. (2a) and (3a) are thus reduced to

$$\varphi_1 = -u_\infty x + A_1 e^{\alpha x} J_o(\alpha r) \quad (2b)$$

$$u_r = A_1 e^{\alpha x_i} \alpha J_1(\alpha r) \quad (3b)$$

The bubble profile in the neighborhood of stagnation point $x_i(r)$ in steady-state was evaluated (Ref. (2)) from the condition of zero streamline function

$$\Psi_r(x_i, r) = -\frac{U\rho}{2} r^2 + A_1 r e^{\alpha x_i} J_1(\alpha r) = 0 \quad (5)$$

In this study, a disturbance is superimposed on the stationary condition developed in Ref. (2). The disturbance part of the velocity potential is assumed to be

$$\varphi_2 = \sum_m A_{2m} e^{iw_m t} e^{k_m(x-x_i)} J_o(k_m r) \quad (6)$$

Where k_m is the m^{th} wave number and w_m is the m^{th} frequency. Such a form is selected so that $\varphi_2 \to 0$ as $x \to -\infty$ to satisfy the boundary condition, and $J_o(kr)$ is used to satisfy the LaPlace equation $\nabla^2 \varphi = 0$ in cylindrical coordinates. In Eq. (6), the use of $J_o(k_m r)$ is based upon the assumption of axisymmetry.

By combining the steady-state velocity potential with the perturbation velocity potential, the velocity potential for the liquid around a bubble becomes

$$\varphi = \varphi_1 + \varphi_2 \quad (7)$$

For the gas-phase inside a bubble, the steady-state velocity potential is assumed to be zero. Thus, only the perturbation part will exist

$$\varphi' = \varphi_2' = \sum_m B_{2m} J_o(k_m r) e^{-k_m(x-x_i)} e^{iw_m t} \quad (8)$$

Note that φ_2' in Eq. (8) vanish when $x \to +\infty$, to satisfy the boundary condition.

The kinematic condition at the interface is

$$\frac{\partial \varphi'}{\partial x} = \frac{\partial \eta}{\partial t} \qquad \text{in the vapor phase} \quad (9)$$

$$\frac{\partial \varphi}{\partial x} = \frac{\partial \eta}{\partial t} + u_r \frac{\partial \eta}{\partial r} \qquad \text{in the liquid phase} \quad (10)$$

Now, since an instability grows most rapidly at the extrema of the displacement, the mathematics can be simplified if we are only concerned about the extrema where $\partial\eta/\partial r = 0$, then Eq. (10) is reduced to

$$\frac{\partial \varphi}{\partial x} = \frac{\partial \eta}{\partial t} \quad (10a)$$

The disturbance on the interface will be represented by

$$\eta = (x_i - x_{io}) = \sum_m \eta_{o_m} e^{iw_m t} J_o(k_m r) \quad (11)$$

to be compatible with φ and φ' in Eqs. (6) and (8). The pressure at both sides of the interface is assumed to obey Bernoulli's equation, hence

$$p = g(\eta + x_{io})\rho - \frac{\rho}{2}(u_r^2 + u_x^2) + \rho \frac{\partial \varphi}{\partial t} \quad (12)$$

The pressure difference on the two sides of the interface is balanced by interfacial tension. The resulting equation of pressure balance is:

$$\sigma\left[\frac{\partial^2 \eta}{\partial r^2} + \frac{1}{r}\frac{\partial \eta}{\partial r}\right] = g\eta(\rho - \rho') - \rho\left(\frac{\partial \varphi_1}{\partial r}\right)\left(\frac{\partial \varphi_2}{\partial r}\right)$$
$$- \rho\left(\frac{\partial \varphi_1}{\partial x}\right)\left(\frac{\partial \varphi_2}{\partial x}\right) + \rho \frac{\partial \varphi_2}{\partial t} - \rho' \frac{\partial \varphi_2}{\partial t} \quad (13)$$

The combination of Eqs. (2) to (13) results in an equation for the wave period w_m. The stability criterion for a bubble is that the wave will not grow with time, or mathematically, that the wave period w_m should have no positive real part in the root. This condition is equivalent to

$$k_{am} > k_{am}^* = \sqrt{\frac{\Delta \rho g}{\sigma}} \quad (14)$$

Since the smallest root of the Bessel function $J_o(k_m a)$ is $k_{a1} a = 3.832$

$$a \le a^* = 3.832\sqrt{\frac{\sigma}{g\Delta\rho}} \quad (15)$$

For an air-water system the critical size is

$$a^* = 1 \text{ cm}$$

For a N_2-CCl_4 system, the critical size is

$$a^* = 0.46 \text{ cm}$$

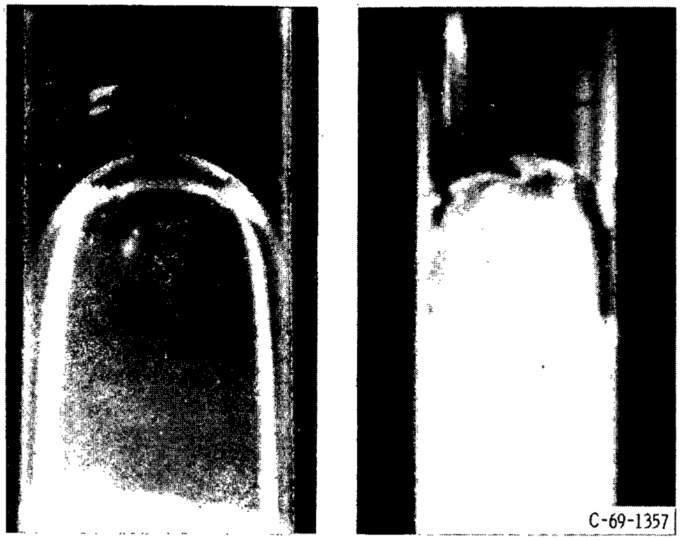

(a) Stable. (b) Unstable.

Figure 1. Typical bubbles.

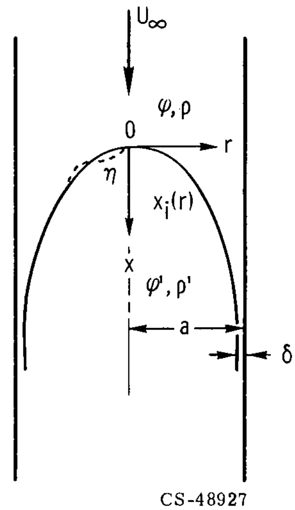

Figure 3. - Coordinates and flow model.

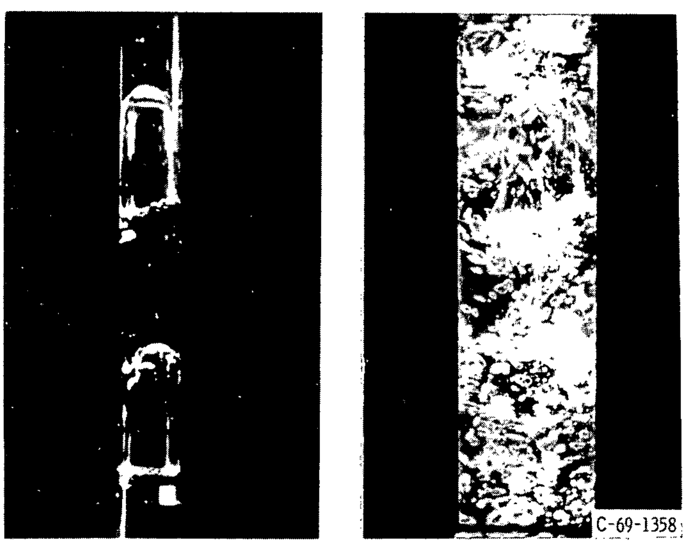

(a) Stable. (b) Unstable.

Figure 2. - Typical slug flow.

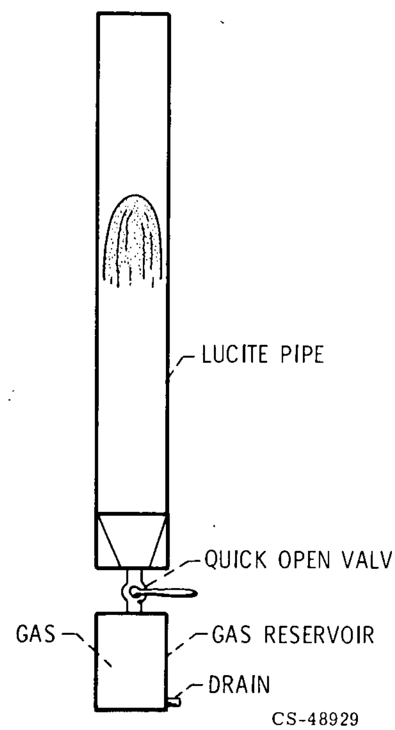

Figure 4. - Apparatus (on ground).

EXPERIMENTAL STUDY OF A SINGLE BUBBLE

Experimental Setup

Test were carried out for pipes of various sizes ranging from 1.27 cm to 25.4 cm in diameter.* The apparatus is shown in Fig. 4. The basic components were a transparent pipe to hold the liquid column and a gas reservoir chamber. The pipe height was about 20 to 30 times the respective diameter. The liquids used were mostly water, with a few runs of carbon tetrachloride. The air or nitrogen gas was introduced from the reservoir through a quick-opening valve. The reservoir was connected to a supply of gas through a regulating valve so that the gas pressure could be maintained at any desired level. For large pipes a fine screen and a cone shaped entrance section were provided at the bottom of the column to ensure even distribution of gas.

Results and Discussion

The single bubbles were introduced under two kinds of conditions: those introduced into a quiescent liquid, void of disturbance, and those introduced into a liquid with disturbances. For the former case, a liquid column was given a long calming period before a new bubble was introduced. Also, the motion of the liquid was visually checked by the use of tracers to insure no discernable motion was present. For the liquid with disturbances, three types of disturbances were noted: (a) pressure pulsations; (b) convective cells; and (c) bubble wakes. Each of these cases will be discussed individually.

A. Single bubble without disturbance: When a single bubble was introduced into a liquid column without disturbance, the bubble maintained its stable form, while rising to the top of the column. This is true for all the pipes up to 25.4 cm (and a few bubbles in a pipe of 35.6 cm in diameter. Unfortunately, this pipe broke before more data could be taken with it).

Such persistance of a stable configuration of a Taylor bubble in pipes much bigger than the analytically predicted critical pipe diameter was surprising. The discrepancy between the analytical and experimental result might be due to one of two possible reasons: (1) The small perturbations that naturally exist in a quiescent flow would need time to grow. Since in the present study a bubble rose to the top of a column in a time span of about 10 to 20 seconds, the time might be too short for the perturbation to grow into an appreciable magnitude. The analysis only gives a stability criterion but does not specify how soon the instability will set in. To determine the rate of growth of instability, more analysis is needed. (2) It was observed that, sometimes, a small deformation would develop at the interface, and as the bubble was rising, the flow field around the bubble would sweep the deformation to the side of the bubble before it could cause instability. This observation might indicate that the displacement should be expressed in some form other than that of Eq. (11), which is a result of the simplification of Eq. (10a).

It will be shown later that although the bubble stability criterion failed to predict the result of single bubbles in a quiescent flow, over the time span of 10 to 20 seconds, the criterion is still useful.

B. Single bubble with disturbances: Since the single bubbles remained stable in a quiescent flow during the residence time in a pipe, it is interesting to observe the effect of a disturbances on the bubble stability. As mentioned previously, three types of disturbance were imposed:

1. Pressure pulsation: When a bubble was introduced into a liquid column from a gas reservoir with a pressure somewhat higher (say, 1/3 atmosphere higher) than that at the base of the column, the bubble would go through expansion and contraction cycles. The pressure pulsation was dramatized by the appearance and disappearance of fog in the bubble (Fig. 5). The bubble nose and the liquid in front of it went through acceleration and deceleration stages. The body force and the flow field apparently were so affected that bubble instability was readily observable. This instability was observed for all the pipe diameters down to 5 cm in diameter.

2. Convective cell: When the liquid in one section of the column was warmer than the rest or when ice was floated at the top of the column (Fig. 6), an inverted density gradient was present which caused convective circulation. The convective cell was made visible through the use of fine tracer particles. This test was carried out only in the 25.4 cm diameter pipe. (In the movie, the sequence with tracers was filmed at 12 frames per second to dramatize the motion of the circulation.) It was observed that the bubble broke up whenever it passed through the circulation region. For the ice-cooled column, the density-inversion zone diffused downward gradually from the top. Consequently, the location of the bubble instability also shifted downward each time a new bubble was introduced.

3. Wake effect: When a Taylor bubble rises, a wake is formed behind the bubble. This is shown in Fig. 7. It appears to have two regions: (1) a strong wake region, of 3 to 5 diameters long and (2) a weak wake region beyond the strong wake region.

*For the large pipes, preliminary tests were carried out by using stove pipe construction (diameter 18 cm to 25 cm) rolled from 1 mm thick clear plastic sheets. These pipes were put vertically in a swimming pool (5.6 m deep). The near balance of the hydrostatic heads inside and outside of the underwater pipe enabled the use of thin-walled pipes. An inflated balloon was pulled in a net to the bottom end of the pipe and allowed to rise slowly. The rising balloon was punctured by a needle to release the air and a Taylor bubble was formed. The activity of the Taylor bubbles were recorded using an underwater camera. The Taylor bubbles, even in large pipes, were found to be both stable and unstable, depending upon the test conditions. The preliminary study showed that more interesting and meaningful results could be expected if tests were conducted under more controlled conditions. Consequently, thick-walled plastic or glass pipes of various diameters were used for more tests.

As a trailing bubble was introduced into the wake region, the bubble was stable or unstable depending upon the spacing time (or spacing length) between the two bubbles. The situation is rather complicated. In order to obtain a more definitive view of the wake effect, the bubble interaction is studied more closely in the next sections.

ANALYSIS OF BUBBLE INTERACTIONS

Since the effect of a preceding bubble on a trailing bubble is transmitted through its wake vorticity, it is logical to first study the decay of the wake vorticity.

Consider the situation at a given location, the wake vorticity gradually decays with time due to viscous dissipation. The attenuation of vorticity can be expressed as (Ref. (22), p. 54)

$$\frac{D\Omega}{Dt} = \nu\nabla^2\Omega \tag{16}$$

Since there is no net flow in the liquid after the bubble has passed, the equation can be simplified to read

$$\frac{\partial\Omega}{\partial t} = \nu\nabla^2\Omega \tag{16a}$$

The boundary conditions are

$$\begin{aligned} \Omega &= \Omega_o \text{ at } t = 0 \\ \Omega &= 0 \text{ at } r = R \end{aligned} \tag{17}$$

The solution can be found in Ref. (23) by Carslaw and Jaeger.

$$\frac{\Omega}{\Omega_o} = \frac{2}{a}\sum_{n=1}^{\infty} e^{-\nu t/r^2 c_n^2} \frac{J_o(c_n\frac{r}{a})}{\frac{c_n}{a} J_1(c_n\frac{r}{a})} \tag{18}$$

Inspection of Eq. (18) reveals the decay ratio Ω/Ω_o is the same if the parameter $\nu t/a^2$ or $\nu t/D^2$ does not change. Now we may hypothesize that there exists a critical vorticity ratio $(\Omega/\Omega_o)_c$ which is strong enough to initiate the instantaneous instability at the nose of the Taylor bubble. This assumption implies a critical parameter $(\nu t/D^2)_c$ so that for a given pipe diameter and fluid viscosity, there is a critical spacing interval t_c between two consecutive bubbles. If the second bubble is introduced after the t_c, the wake effect is sufficiently decayed and the bubble instability cannot be tripped instantaneously.

EXPERIMENTAL RESULTS OF BUBBLE INTERACTION

The same apparatus described previously was used for the bubble interaction study. The procedure was the same except that the spacing between two consecutive bubbles was controlled and recorded. During the test for the large pipes (> 10 cm), a leading bubble was first introduced, then a second bubble was introduced at a preset time spacing. The camera was activated to follow the motion of the second bubble. For small pipes, it was more convenient to introduce two bubbles at close sequence and the spacing time was determined from the spacing length recorded by the motion picture through the relation

$$t_c = \frac{L_c}{u_b}$$

The critical spacing between bubbles was taken when a trailing bubble just began to show instability somewhere on its nose.

Results and Discussion. - For a given pipe diameter, there is a narrow range of critical spacing: for spacings less than critical the bubble was always unstable, and for spacings larger than critical the bubble was always stable. Within the narrow range of critical spacing (or marginal spacing), the result was statistically random. In general, the result is: (a) The bubbles in pipes of subcritical size were stable in the weak wake but deformed or merged with the preceding bubble once they reached the strong wake region: (b) The bubbles in the pipes of critical size were stable in the weak wake region but broke down upon reaching the strong wake region. This was observed for both water-air and CCl_4-N_2 systems. The strong wake region length could vary anywhere between 3 to 5 diameters. (c) For bubbles flowing in pipes larger than the critical size, the bubble began to breakup even in the weak wake region. The critical spacing increases with pipe diameter.

If we take the product of the kinematic viscosity and the experimental values of the spacing interval for marginal stability of the trailing bubble, and plot this product against diameter, it should result in a line of

$$\nu t_c = CD^2 \text{ or } \frac{\nu t_c}{(\nu t_c)_o} = \left(\frac{D}{D_o}\right)^2 \tag{19}$$

Where the subscript o refers to some reference condition. The comparison of the experimental result with Eq. (19) is shown in Fig. 8.

Equation (19) shows that the critical spacing time t_c for the bubble in a pipe diameter D can be scaled if the values of t_o and D_o at some reference condition are available. However, recall the data for bubble stability inside pipes of critical diameters for both water-air systems and CCl_4-N_2 systems. In both cases, instability sets in when the trailing bubble entered the strong wake region, which was observed to be about 3 to 5 diameters long. It was interesting to note that the strong wake region corresponds favorably with the region of large enhancement of velocity of the trailing bubble as reported in Ref. (18) and shown in Fig. 9. In this figure, again the wake effect was near the tail but quickly declined to small values within the separation distance of 3 to 4 diameters. Therefore, it is logical to use the critical pipe diameter D^* and the spacing of the strong wake region $L_w/D = 4$ or $t_c^* = 4D^*/u_b$ as the reference condition t_o and D_o. The resulting correlation for critical spacing is

$$t_c = \frac{\nu_o}{\nu}\left(\frac{ND^*}{u_b^*}\right)\left(\frac{D}{D^*}\right) \tag{20}$$

Where $N = 4$ for the present study, and it might be a function of fluid properties and pipe geometry if the con-

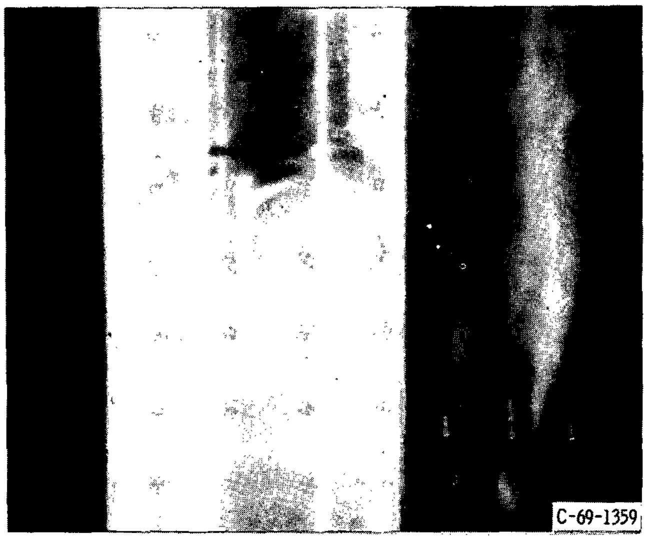

Figure 5. - Bubble under pulsating condition. (Note the fog inside the bubble.)

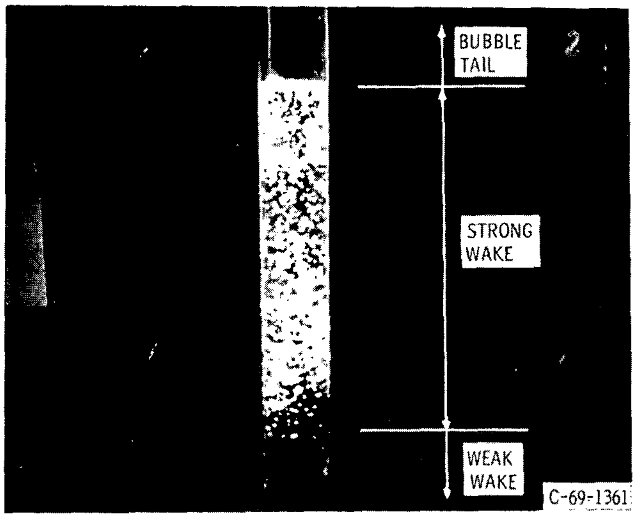

Figure 7. - Wake regions behind a bubble.

Figure 6. - Convective cells in the inverted density - gradient zone.

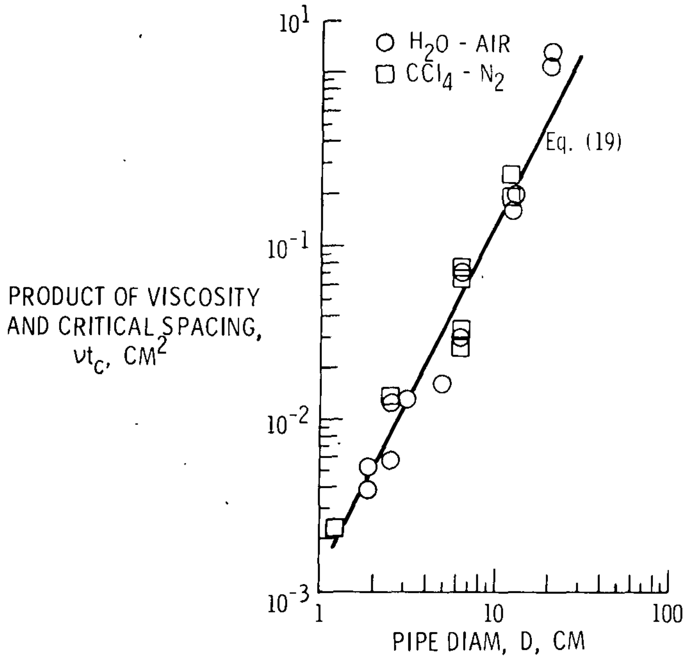

Figure 8. - Critical spacing as a function of diameter.

dition is considerably different from what was encountered in the present study.

Implication of Correlation to Slug Flow

The correlation of critical spacing time t_c and the corresponding critical spacing length $L_c = t_c u_b$ serves as a limit to slug flow stability. The implications are: (1) If the intermittancy of bubbles admitted into a two-phase flow is less than the critical spacing time, no stable slug flow can exist. The trailing bubbles will breakdown and form churned bubbly flow. (2) If the bubble length L_b is known, then the void fraction $\alpha = L_b/(L_b + L_L)$ of a slug flow should be limited by the value $L_b/(L_b + L_c)$ since L_L should be less than L_c (3) For a pipe length L_p, if $L_p > L_c$ there cannot be two consecutive bubbles flowing simultaneously in the pipe, and therefore slug flow cannot be expected.

CONCLUSION

The stability of Taylor bubbles in pipes of diameters ranging from 1.27 cm to 25.4 cm was studied. The pipes were 20 to 30 diameters long. Both air-water and N_2-CCl_4 bubbles were studied. The findings can be summarized as:

1. For a single bubble in a quiescent liquid column, the critical size for a stable bubble was predicted to be $3.832\sqrt{\sigma/\Delta\rho g}$ from a small-perturbation analysis. But bubbles in pipes 12 times larger than the critical size were found to remain stable, at least for the duration of their residence time which was of the order of 10 to 20 seconds.

2. For bubbles flowing in a liquid column the following imposed disturbances were considered:
(a) pulsating bubbles
(b) convective cells
(c) wakes of bubbles
The bubble was unstable under those conditions.

3. A quantitative study of wake effects in pipes showed that:
(a) For bubbles less than the critical size, the bubbles were stable unless they happened to be inside the strong wake region. If so they soon merged with the leading bubble.
(b) For the pipe of critical size, the bubble was stable throughout the weak region but broke up at the entrance to the strong wake region.
(c) For the pipes larger than the critical size, the bubbles broke up at a distance (or interval) from the leading bubble. The critical spacing time increases roughly with square of the diameter. It can be correlated using Eq. (19).
(d) A stable slug flow cannot be maintained if the spacing between bubbles is less than the critical value. Such information sets a limit for the stable operation of slug flow.

REFERENCES

1. G. Taylor, "The Instability of Liquid Surfaces When Accelerated in a Direction Perpendicular to Their Planes I," Proceedings of the Royal Society (London), Ser. A, vol. 201, no. 1065, March 22, 1950, pp. 192-196.

2. R. M. Davies and G. Taylor, "The Mechanics of Large Bubbles Rising Through Extended Liquids and Through Liquids in Tubes," Proceedings of the Royal Society (London), Ser. A, vol. 200, no. 1062, February 7, 1950, pp. 375-390.

3. D. T. Dumitrescv, "Flow Past an Air Bubble in a Vertical Pipe," Zeitschrift fuer Angewandte Mathematek und Mechanik, vol. 23, 1943, pp. 139-149.

4. P. Griffith and G. B. Wallis, "Two-Phase Slug Flow," Journal of Heat Transfer, vol. 83, no. 3, August, 1961, pp. 307-320.

5. G. Birkhoff and D. Carter, "Rising Plane Bubbles," Journal of Mathematics and Mechanics, vol. 6, 1957, pp. 769-779.

6. P. R. Garabedian, "On Steady-State Bubbles Generated by Taylor Instability," Proceedings of the Royal Society (London), Ser. A, vol. 241, no. 1226, August 20, 1957, pp. 423-431.

7. R. Collins, "A Simple Model of the Plane Gas Bubble in a Finite Liquid," Journal of Fluid Mechanics, vol. 22, pt. 4, August, 1965, pp. 763-771.

8. R. Collins, "The Effect of a Containing Cylindrical Boundary on the Velocity of a Large Gas Bubble in a Liquid," Journal of Fluid Mechanics, vol. 28, pt. 1, April 12, 1967, pp. 97-112.

9. G. I. Taylor, "The Formation of Emulsions in Definable Fields of Flow," Proceedings of the Royal Society (London), Ser. A, vol. 146, no. 858, October 1, 1934, pp. 501-523.

10. R. A. S. Brown, "The Mechanics of Large Gas Bubbles in Tubes. I. Bubble Velocities in Stagnant Liquids," Canadian Journal of Chemical Engineering, vol. 43, October, 1965, pp. 217-223.

11. F. P. Bretherton, "The Motion of Long Bubbles in Tubes," Journal of Fluid Mechanics, vol. 10, pt. 2, March, 1961, pp. 166-188.

12. H. L. Goldsmith and S. G. Mason, "The Flow of Suspensions through Tubes. II. Single Large Bubbles," Journal of Colliod Science, vol. 18, 1963, pp. 237-261.

13. J. R. Street and M. R. Tek, "Dynamics of Bullet Shaped Bubbles Encountered in Vertical Gas Liquid Slug Flow," AICHE Journal, vol. 11, no. 4, July, 1965, pp. 644-650.

14. D. J. Nicklin, J. O. Wilkes, and J. F. Davidson, "Two-Phase Flow in Vertical Tubes," Transactions of the Institute of Chemical Engineers, vol. 40, 1962, pp. 61-68.

15. A. J. Nicolitas and W. Murgatroyd, "Precise Measurements of Slug Speeds in Air-Water Flows," Chemical Engineering Science, vol. 23, 1968, pp. 934-936.

16. I. Slaughter, and A. E. Wraith, "The Wake of a Large Gas Bubble," Chemical Engineering Science, vol. 23, 1968, p. 932.

17. J. K. Walters and J. F. Davidson, "The Initial Motion of a Gas Bubble Formed in an Inviscid Liquid. Part 2, The Three-Dimensional Bubble and the Torodial Bubble," Journal of Fluid Mechanics, vol. 17, pt. 3, November, 1963, pp. 321-336.

18. R. Moissis and P. Griffith, "Entrance Effects in a Developing Slug Flow," MIT Report DSR 7-7673, Tech. Rept. No. 18, 1960.

19. R. Moissis, "The Transition from Slug to Homogeneous Two-Phase Flows," Journal of Heat Transfer, vol. 85, no. 4, November, 1963, pp. 366-370.

20. R. Bellman and R. H. Pennington, "Effects of Surface Tension and Viscosity on Taylor Instability," Quarterly of Applied Mathematics, vol. 12, 1954, pp. 151-162.

21. Y. Y. Hsu and F. F. Simon, "Stability and Interaction of Cylindrical Bubbles in a Vertical Pipe," Proposed NASA Technical Note.

22. H. Schlichting, Boundary Layer Theory, McGraw-Hill Book Company, Inc., New York, 1955, p. 54.

23. H. S. Carslaw and J. C. Jaeger, Condution of Heat-in Solids, 2nd ed., Oxford Press, London, 1959, p. 199.

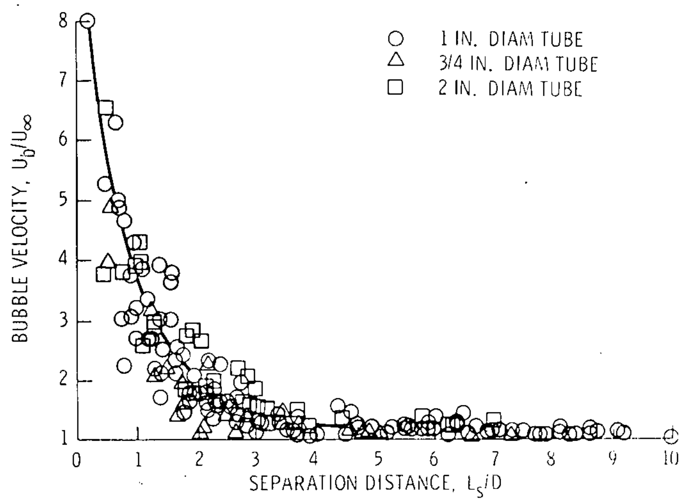

Figure 9. - Velocity-separation distance data (ref. 18).